

36 1947, and more than 470 people died due to slope failures and debris flow associated with man-
37 made cut slopes, fill slopes and retaining walls.

38 There are many reported serious slope failures and debris flow problems in China in the recent ten
39 years, due to the significant amount of constructions and inadequate stabilization to many
40 temporary or permanent fill or natural slopes. The destructive power of large scale debris flow is
41 well known, and the prevention of slope instability, reduction of debris flow destructive power by
42 the use of rigid, flexible barrier or other means are well practiced in many countries. There are
43 many cases where the slopes fail with subsequent debris flows in Hong Kong and China (Scott
44 and Wang 1997), which have created various serious problems. Based on a conservative estimate,
45 over 60 countries in the world have faced the problems of debris flow over the years. With
46 reference to Fig.1, the debris flows in Hong Kong and China have created traffic problems, serious
47 loss of lives and properties, and currently there are many active research works in the area of debris
48 flow in Hong Kong and China. The research works include three-dimensional slope stability
49 analysis, debris flow process, impact loads on flexible and rigid barriers and others. An example
50 on three-dimensional slope stability analysis using 16000 columns has been carried out by Cheng
51 in 2016/2017 which is shown in Fig.2a (Lo et. al. 2018). The analysis of the non-spherical surface
52 is achieved by the use of Nurbs function as discussed by Cheng et al. (2005). Upon the
53 determination of the critical failure mass, and the flow path of the soil can be estimated from a
54 distinct element analysis using the method as discussed by Cheng et al. (2015). The slope failure
55 and the subsequent debris flow (2100m³ of debris) as shown in Fig.2b is finally protected by the
56 use of three levels of flexible barrier against the future potential debris flow. The authors are also
57 considering the use of meshless method in the assessment of debris flow, which will be the next
58 stage of the present work (Wong 2018).

59

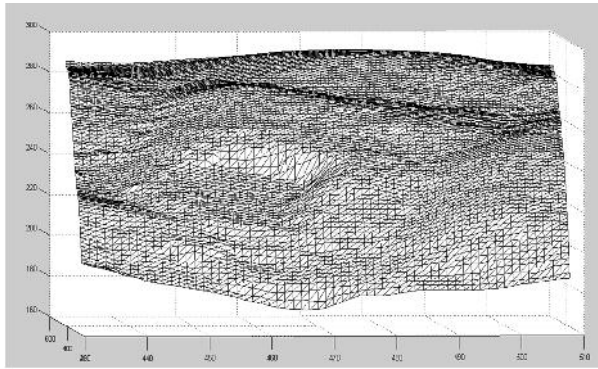


60
61 (a)



(b)

62 Fig.1 Representative debris flow in Hong Kong and Shenzhen, China (a) Tsing Shan debris flow
63 in 1990 (King 2013); (b) debris flow in Shenzhen 2015 (see Wikipedia).



64

65

(a) 3D slope stability analysis

(b) Debris flow after slope failure

66 Fig.2 Three-dimensional slope stability analysis by Cheng (the triangulation represent the
 67 geometry as defined by the GIS information) and the subsequent debris flow for a slope in Hong
 68 Kong has blocked the Sai Wan Road traffic

69

70 Granular flow as a pilot study of debris flow has some fundamental difficulties in the physical tests
 71 as well as numerical analysis. In general, various particles sizes will be present in a flow, and the
 72 debris mix is usually far from uniform in composition. For physical tests, it is difficulty to apply a
 73 representative debris flow mix, and the flow process is further complicated by the presence of
 74 water. For numerical simulation, it is virtually impossible to accommodate too much particles in a
 75 model, ranging from a very small particle size to cobbles or even boulder in the extreme range.
 76 Even if such a numerical model can be established, there will be serious numerical problems if the
 77 particles sizes differ too much in the system. Granular flow can be induced from gravity, driven
 78 by fluid dynamic or from both factors. The classification of debris has been given by Varnes (1978),
 79 and later modified by Furuya (1980), Ohyaigi (1985), Pierson and Costa (1987), Coussot and
 80 Meunia (1996), Cruden and Varnes (1996), Hungr et al. (2001), Takahashi (2001, 2006) and others.
 81 A detailed theoretical treatment of dry granular flow similar to some of the single material tests in
 82 the present study has been given by Takahashi (2014) and will not be repeated here. In this study,
 83 we will concentrate mainly on the action of gravity, while the effects of water is under study by
 84 the authors as the next stage of research work.

85 Many scientists have carried out granular flow analysis. Lo (2004) has compared the different
 86 composition of granular flow in landsides in Hong Kong and examined the coarse and fine particle
 87 concentration. Hutter et al. (2005) has considered the flow envelopes and the deposition of the flow.
 88 In year 1991, the U.S. Geological Survey has made a large scale flume for detailed experimental
 89 tests on debris flows. Mizuyama and Uehara (1983) have made a flume which is 20 cm wide and

90 25m long, and the slope angle ranged from 5 degree to 25 degree. Liu (1996) has made a 18 cm
91 depth, 16 cm width and 150 cm length flume in Yunnan, China, and the flume inclination can be
92 adjusted from 10 to 34 degrees. Lin (2009) has made a 20 cm width 8m length flume with a 2.2 m
93 width 3 m length catchment. There are also various flume tests that have been carried out by
94 various researchers in Hong Kong and many other countries.

95 During the transportation period, segregation occurs when debris starts to flow. Iverson (1997)
96 studied the factors that influence the segregation process. He found that particle size has a great
97 effect on the segregation process, and debris with larger particle size move upward while fine
98 particles go downwards. This phenomenon is the opposite of “normal grading” in which the finer
99 particles are found at the upper layers in the lake or river and large particles rest at the bottom. The
100 main reason for the segregation is kinetic sieving, and finer particle can go through the gaps
101 between particles more easily than the larger particle. Large particles can also be found at the front
102 of the flow because of the relatively high velocity of the larger particles at the upper layer,
103 compared with the finer particles with lower velocity at the lower layer. When a stable contact
104 network for large particle is formed at the free surface, the segregation cease to occur and the balls
105 finally deposit at the catchment area.

106 For distinct element modeling (DEM) of granular flow, Jiang et al. (2003) has studied the methods
107 of generations of ball in PFC2D (Cundall 1971, 1988, Cundall and Hart 1992, Cundall and Strack
108 1979), namely the expansion method and isotropic compression method. Zohdi (2007), Halsey and
109 Mahta (2002) discussed about the physics of granular flow; the contact model and the limit of the
110 friction coefficient. Sullivan (2011) also compared the theory and computation in distinct element
111 analysis. It is well known that the use of DEM can only provide qualitatively instead of quantitative
112 study up to the present (see also the discussion part), and most researchers adopt DEM for
113 qualitative analysis only.

114 In the present study, dry granular flow experiments will be conducted under different conditions
115 using glass and rubber balls for a basic study on the flow process and segregation. Both glass and
116 rubber balls of different diameters have been used in the tests, and combination of different size
117 and materials have also been tried in the tests for the illustration of the segregation problem. The
118 experimental results are also analyzed by distinct element analysis using program PFC2D. It is
119 true that three-dimensional distinct element modelling can be a better tool for the present problems,
120 but the previous experience in three-dimensional distinct element modelling by the authors suggest
121 that the amount of computer time can be significant. For the present study, the flume in both the
122 laboratory and field tests are relatively narrow, and off-track movement of the balls/grains are not
123 major. In view of that, two-dimensional modelling has been adopted in the present study, and good
124 results are actually obtained. The tests are performed at relatively simple condition so that the basic
125 problem of flow and segregation can be studied easily. It should also be mentioned that more than
126 10 ten thousands photos are taken from the laboratory and field tests, and such amount of
127 information cannot be fed into a paper. In views of that, only representative intermediate photos

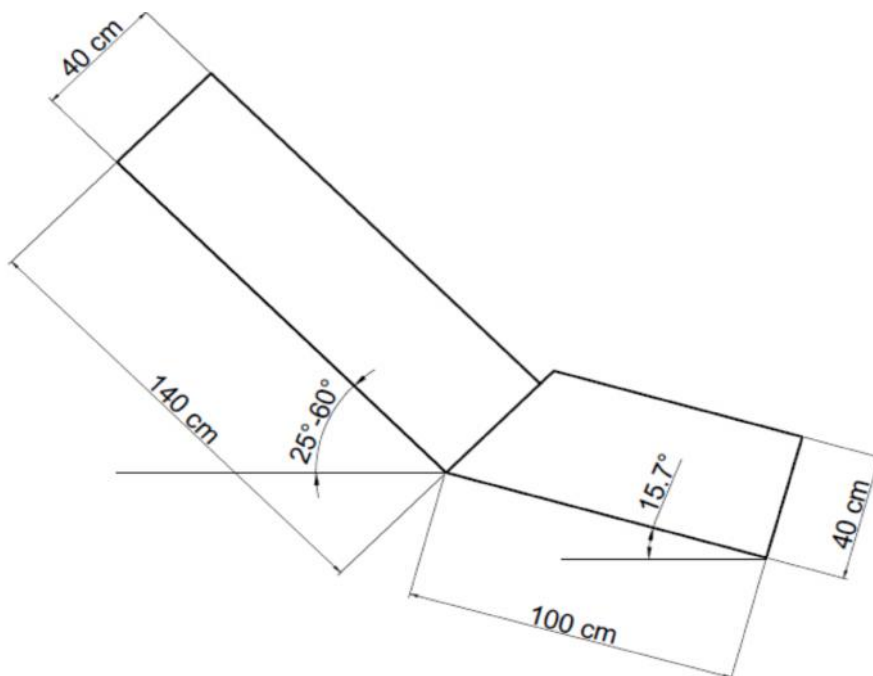
128 which are used for illustration are given in the present paper, while some of the observed
129 phenomena are simply description without the support of the photos.

130

131 **2. Physical flume modeling of granular flow**

132 **2.1 Instrumentation and Test Material**

133 To enhance the knowledge on the granular flow mechanism, many laboratory and large scale field
134 tests have been carried out by the authors. The laboratory model is about 1.5m long and 1.3m high
135 (adjustable). The flume in the laboratory is made of polystyrene and is designed to be flexible, and
136 the angle of inclination can be adjusted if necessary. The flume model is 40cm depth, 40 cm width,
137 140 cm length of upper flume and 100 cm for the lower flume with a 60 x 60 catchment area at
138 the bottom. Fig. 3 and Fig 4 show the schematic design of flume and flume model in the laboratory
139 tests. In order to record the motion of the particles, two high speed cameras are adopted. The first
140 one is mounted on the upper flume while the second one is fixed to the bottom flume. In the
141 laboratory tests, different sizes of glass beads and rubber beads are used to replace the use of sand,
142 and this simplification can help to assess the effects of shape and material on the segregation
143 process. In the large scale field test, real sand is used. For the material parameters, the dynamic
144 friction angle is measured by using tilting test (Pudasaini & Hutter (2007), Mancarella & Hungr
145 (2010)). The property of the glass and rubber beads are determined experimentally, and the details
146 are given in Table 1.

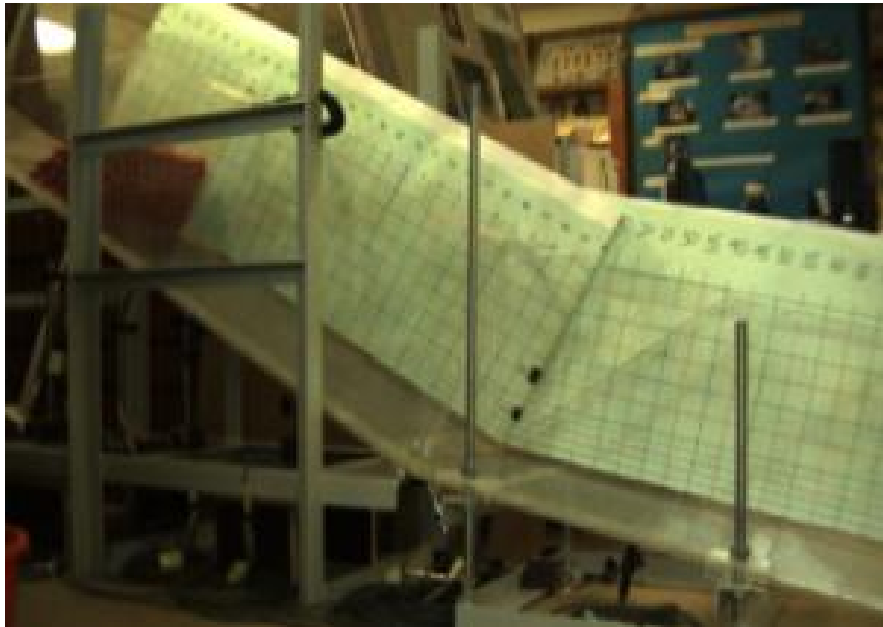


147

148

Fig.3 Schematic Design of Flume

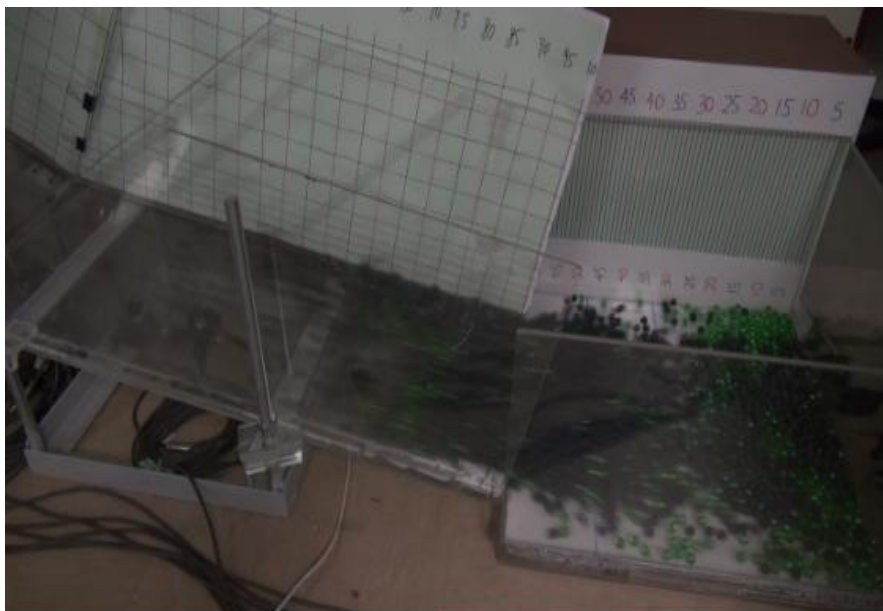
149



150

151

Fig.4 Flume model in laboratory



152

153

Fig 5. Flume model with a small jump in laboratory



154

155 Fig.6a Transparent glass



Fig.6b Blue glass ball



156

157 Fig.6c Green glass ball



Fig.6d White plastic ball



158

159 Fig.6e Red plastic ball



Fig.6f Black plastic ball

160

161 Table 1. The properties for the glass balls and plastic balls in laboratory granular flow test

Plastic	D(mm)	Average Weight	Density (kg/ m ³)	External Friction Coefficient	Internal Friction Coefficient
White	50	105.35	1609.64	0.781	0.547
Red	30	23.382	1653.97	0.630	0.429
Black	15	2.862	1619.56	0.222	0.365
Glass	D(mm)	Average Weight	Density (kg/ m ³)	External Friction Coefficient	Internal Friction Coefficient
Transparent	40	78.686	2348.11	0.102	/
Blue	25	21.121	2581.64	0.053	/
Green	16	5.744	2678.28	0.104	/

162

163 2.2 Test Programme

164 In the present study, the angle of the flume in laboratory is kept to be 45 degree. The effect of the
165 slope inclination will not be discussed in this paper, but the test results by the authors show that
166 the segregation process will basically remain unchanged with different flume inclination. The
167 effect of flume inclination can affect the degree of segregation as well as impact forces which will
168 be covered by a separate paper later. Totally 68 laboratory tests have been carried out. The 68 tests
169 are divided into two groups: the first group of tests were conducted on the flume with a small jump,
170 and the other group of tests were carried out on the flume without a jump. Such a jump is also
171 commonly adopted in Hong Kong, and this helps to lower the velocity of the granular flow (for
172 small scale flow). Fig 5 shows the flume in laboratory with a small jump. The effects of the particle
173 size and the flowing mass are also studied through the use of balls with different diameter, mass
174 and combination of different balls. Table 2 shows only some of the test programme. Test 1 to test
175 48 belong to the first tests group with a small flume jump. Test 1 to test 6 were carried out by using
176 six different kinds of balls separately with the same mass of 10 kg. The mass of the balls is then
177 changed to 13.55kg and the above tests are repeated again (for test 7 to 10). In order to study the
178 segregation process for test 11 to 40, two kinds of balls with different diameters were combined
179 together, and for the same purpose in test 40 to test 48, three kinds of balls were combined together.
180 Test 49 to test 68 belong to the group without a small flume jump. Same as the first group of tests

181 with a small flume jump, test 49 to test 55 were carried out for same material but different sizes of
 182 balls. In test 56 to test 63, combinations of two kinds of balls were tried. The last five tests were
 183 the combination of three kinds of balls.

184

185 Table 2. Test Programme

Flume with a small jump					
One kind of balls	Test Number		Flow Mass		Balls
	1		10 Kg		G(Transparent)
	2		10 Kg		P(White)
	7		13.55Kg		G(Green)
Two kinds of balls	8		13.55Kg		P(Red)
	Test Number		Top Layer		Bottom Layer
	11		P(White)		P(Red)
Three kinds of balls	26		G(Trans)		P(White)
	Test Number	Top Layer	Middle Layer	Bottom Layer	
	41	P(White)	P(Red)	P(Black)	
	45	G(Trans)	P(Red)	P(Black)	

186

Flume without a small jump					
One kind of balls	Test Number		Flow Mass		Balls
	49		10 Kg		G(Transparent)
	50		10 Kg		G(Blue)
Two kinds of balls	Test Number		Top Layer		Bottom Layer
	55		P(White)		P(Black)
	56		G(Trans)		P(Black)
Three kinds of balls	Test Number	Top Layer	Middle Layer	Bottom Layer	
	67	G(Trans)	P(Red)	P(Black)	
	68	G(Trans)	P(Red)	G(Green)	

187 P: P refers to plastic balls, G: G refers to glass beads

188

189 **2.3 Test procedure and test results**

190 Test materials with different particle size combinations (single type of balls to multiple types of
 191 balls) were put into the container which is on the top of the flume. Figure 7 shows the flow pattern
 192 of single type dry granular material flowing along the flume. The video captured by high speed
 193 camera can show this process clearly. When the gate of the container was pulled up, the front part
 194 of flow mass become loose and start to flow along the upper flume under the action of gravity,
 195 while the latter part of flow mass followed behind. Flow mass elongated when it moved forward,

196 and the shape of flow front is wedge-like type. At the moment when the particles reached the
197 bottom of the flume, the velocity direction of the balls changed because of the angle difference
198 between the upper flume and the lower flume. During the transportation period, a large amount of
199 potential energy of the initial flow mass was transferred to momentum energy accompanying by
200 energy dissipation through the grain collision and friction. Particles at the front of the flow
201 reflected back when they impacted on the wall of deposition zone and collided with the subsequent
202 particles immediately, which consumed the residual momentum energy of flow particles. Finally
203 all the particles rested in the deposition zone.

204 In reality, there are sediments and water in a debris flow. The effect of water is complicated and
205 will not be studied in the present work. The grain size distribution is usually not uniform as in the
206 present laboratory tests. Consequently, a good understanding of the particle flow under a mixture
207 of ball sizes is important. Particle size is a vital parameter for the good understanding of multi-size
208 particle flow because it not only has an effect on the flow dynamic, but also influence the energy
209 attenuation during the whole flow process. Furthermore, the tilting test that is mentioned above
210 demonstrates that the dynamic friction angle depends on the particle size, specifically, larger
211 particle size will has smaller dynamic friction angle while smaller particle size will has larger
212 dynamic friction angle. The flow pattern of multi-size particle flow is more complicated when
213 compared with the single size particle flow.

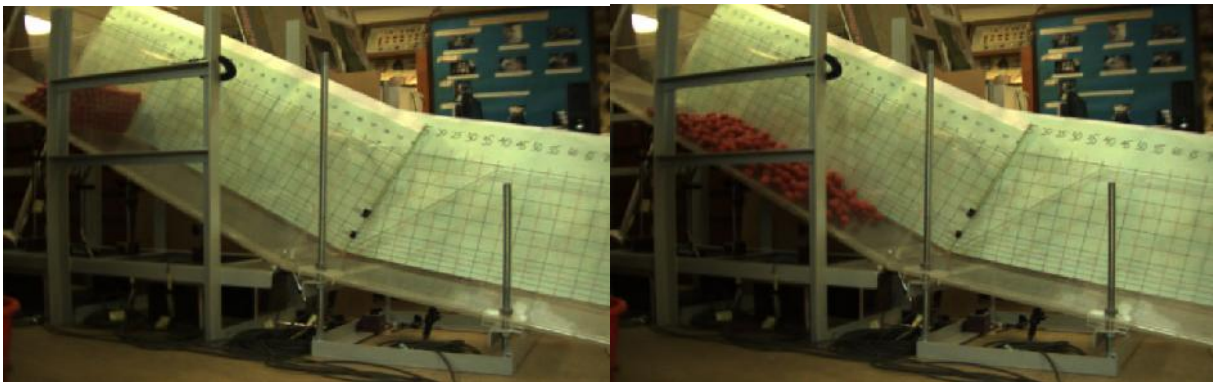
214 Figure 8 shows the flow pattern of multi-size particle flow. Segregation occurred when the
215 combined particles started flowing along the flume. Figure 8a demonstrates the flow pattern of
216 multi-size particle flow composing of white and black plastic balls. The diameter of the white
217 plastic ball is much larger than the black plastic ball as shown in Table 1. From the video captured
218 by the high speed camera, it is easy to observe that during the transportation period, white plastic
219 balls flowed on the upper layer while black plastic balls stayed at the bottom layer. This
220 phenomenon is consistent with the segregation theory of Savage et al. (1988). Besides, it is not
221 difficult to find that white plastic ball always stayed at the front of the flow where the velocity was
222 the highest, in other word, the velocities of the white plastic balls with relative larger diameters
223 are higher than the black plastic balls. Besides, at the upper layer where larger white plastic balls
224 are located, the inertial force dominated the flow dynamic and the energy dissipation was less than
225 that of the lower layer where the flow motion is mainly controlled by the contact forces. For the
226 forgoing reasons, it can be seen that large particle size leads to higher velocity during the flow.

227 Figure 8b shows the flow pattern of multi-size material composing of green glass balls and black
228 plastic balls. The diameter of green glass ball is similar to the diameter of black plastic ball, while
229 the density of green glass ball is almost two times larger than black plastic ball. In the upper
230 container, green glass balls were put statically at the top of the black plastic balls. After pulling up
231 the door, the black plastic balls flowed out firstly at the beginning and stayed at the bottom layer
232 due to the arrangement of the initial position of balls in the container, green glass balls quickly
233 moved downwards under the action of gravity, which leads to the green glass balls at the upper
234 layer replaced by black plastic balls subsequently. When the black plastic balls form a stable

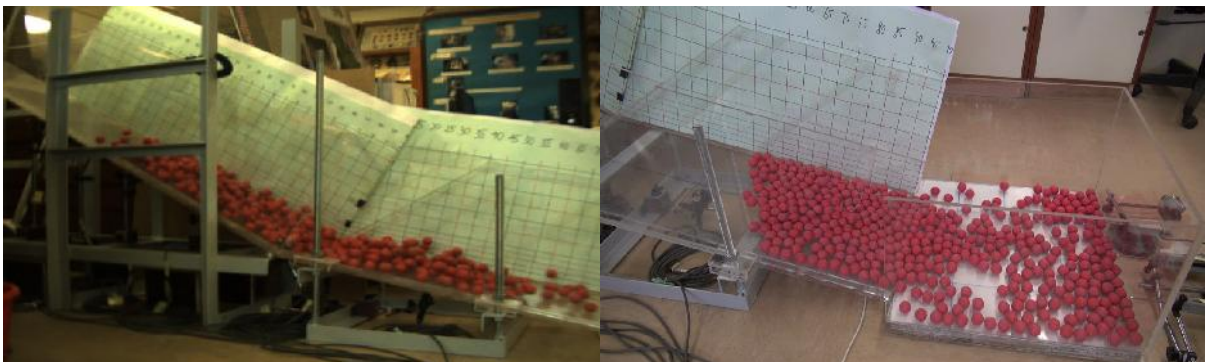
235 contact network at the upper layer of the flow, the position transition or segregation process
236 stopped. In this case, the difference of particle sizes between two kinds of balls is not obvious, and
237 segregation was initiated due to the density difference only. During the segregation process in
238 which green glass balls moved downwards and black plastic balls migrated upwards, the
239 momentums of these two kinds of balls were transferred to each other at neighbor location,
240 therefore green glass balls and black plastic balls arrived at the catchment area almost at the same
241 time, while for the test in which balls were arranged in an opposite order (black plastic balls at top
242 and green glass balls at bottom), the green glass balls move faster and deposit earlier at catchment
243 area compared with the black plastic balls due to the smaller dynamic friction angle as well as the
244 larger kinetic energy of the green glass balls.

245 Similar to the above two figures, Figure 7c shows the flow pattern of transparent glass balls and
246 black plastic balls. In this case, both the density and particle size of the transparent glass balls are
247 larger than that of the black plastic balls. As shown in high speed camera video, during the flow
248 process, the transparent glass balls flow upwards and move faster in comparison with the black
249 plastic balls. Hence, although the density of the transparent glass balls is larger than the black
250 plastic balls, the transparent glass balls still stay at the upper layer of the granular flow due to their
251 relatively large particle sizes, which means that particle size has greater contribution for the
252 segregation process than density in the analysis of granular flow.

253



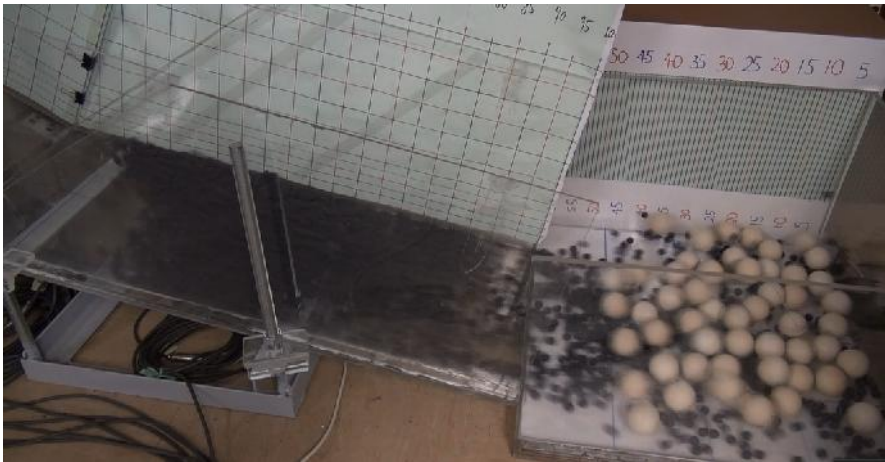
254



255

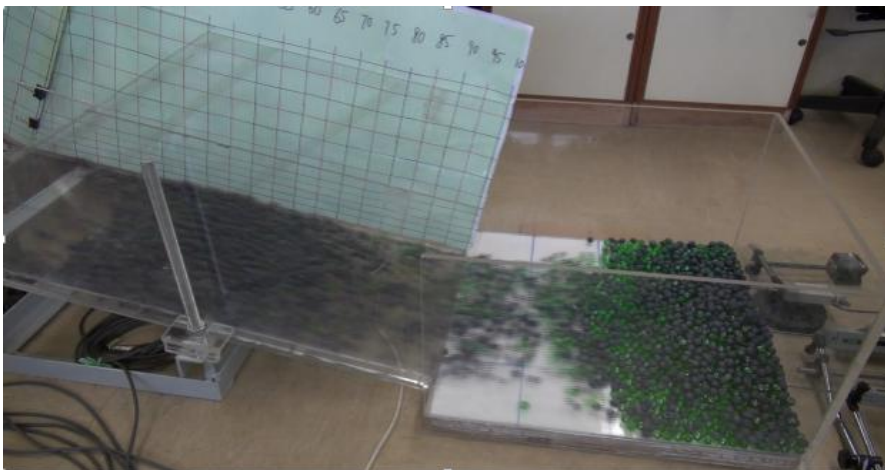
256 Fig. 7. Flow pattern of mono-size particle flow in physical model

257



258

259 a) The influence of particle size on segregation process



260

261 b) The influence of density on segregation process



262

263 c) The influence of particle size and density on the segregation process

264 Fig. 8. Flow pattern of multi-size particle flow

265

266 **3. Numerical Modeling of granular flow**

267 **3.1 Model generation**

268 Previous model tests by Chan (2001) for the runout were calibrated by the Dan model, where the
269 problem of segregation and flume jump were not considered. In general, the results are in
270 agreement with those from Rickenmann (in Jackobs and Hungr 2005). For the present studies
271 where multi-size particles are considered, the use of the simple Dan model is insufficient. The use
272 of meshless method to model debris flow has recently been considered by the authors (Wong 2018).
273 While the meshless method can give a prediction of the debris flow process, the segregation
274 phenomenon is totally neglected in the analysis, but such phenomenon is found to be critical for
275 many cases in Hong Kong. In views of the limitations of these numerical methods, the laboratory
276 tests in the present study are modelled using the distinct element method, which is more
277 appropriate for the large deformation, segregation and separation phenomenon during the
278 transportation process. Once the appropriate numerical model is established, the numerical
279 technique will be extended to the field tests for which natural sand is adopted. In this paper
280 commercial program PFC2D using DEM has been adopted to implement the numerical simulation
281 of dry granular flow. Totally, there are five different methods of model generation in PFC2D
282 program, and based on the consideration of time requirement, the rain method was adopted finally.
283 The parameters used in the numerical simulation are the micro-properties which are difficult to be
284 determined. Benchmark tests have been carried out in order to calibrate the micro-mechanical
285 properties of the dry granular material. Some of the micro-parameters of the balls are determined
286 through changing their values so that the macroscopic behaviors in numerical simulation are
287 consistent with that in physical test. The detailed micro-properties of the balls are shown in Table
288 3. Except for the wall friction (should be small as the walls are relatively smooth) and wall stiffness,
289 all the other parameters in Table 3 are determined by laboratory tests. In order to get different
290 frictional coefficients among the balls, two piece of wood which have plastic balls stick on it
291 regularly and shear force is applied. Furthermore, depositional tests, rebound tests are carried out
292 to measure the frictional angle and rebound coefficients of the balls. For each parameter, five
293 laboratory tests have been carried out, and the mean values are presented in Table 3. It should be
294 noted that there is not a wide distribution in the laboratory determined parameters, hence the range
295 of these parameters are not shown for clarity. The diameters of the particles in the numerical
296 analysis are the same as that used in the physical tests.

297

298 Table 3. Microscopic parameter of the balls for granular flow analysis

Balls	Ball stiffness (N/m ²)	Ball damp	Ball density (kg/m ³)	Ball friction	Wall friction	Wall stiffness (N/m ²)
Red plastic ball	2.36e9	0.4	1250	0.462	0.1	1.11e11
Black plastic ball	7e8	0.2	1250	0.1	0.1	1.11e11
Blue glass ball	7e10	0.3	2500	0.1	0.1	1.11e11
Green glass ball	7e10	0.2	2500	0.1	0.1	1.11e11

299

300

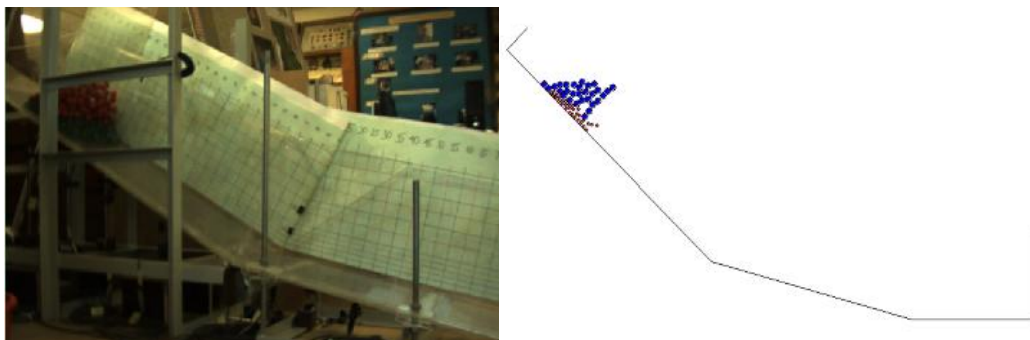
301 3.2 Numerical test results

302 A detailed comparison of the granular flow pattern modeled by the physical tests and discrete
303 element analysis is shown in Figure 9. Figure 9a shows the physical test in which both the red
304 plastic balls and green glass balls were used (too many test results are available, and only selected
305 results are used for illustration in this paper). Large blue balls and small red balls in the numerical
306 model represent the actual red plastic balls and green glass balls in the physical model tests
307 respectively. A full-scale numerical simulation is rare to be conducted for discrete element analysis
308 due to the limitation of the computer resource, but this is considered to be necessary and acceptable
309 for the present study. Figure 9b shows the numerical results of the flow pattern of the multi-size
310 particles. Particles start to flow along the flume after the initiation of the flow. During the flow
311 process, the flow mass became longer under the action of shear force. Particles moved apart from
312 each other and pushed other particles forwards. During this process, the momentums of the balls
313 were exchanged and transferred to other balls at the neighbor locations. The flow velocity keep
314 increasing until the front of the flow hit on the wall of the deposition zone. When the kinetic energy
315 of the balls was exhausted, the balls eventually ceased to move at the catchment area. Figure 10
316 shows the flow pattern of multi-size balls flows composing of black plastic balls and green glass
317 balls of which the diameter are relative smaller than the other balls as considered in the present
318 paper. A pronounced Saltation was observed as balls flowed, implying that the collisional character
319 of the flow mass where the savage number is larger than 0.1 (if the savage number is smaller than
320 0.1, the flow belongs to frictional flow, Iverson 1997). Savage number is the ratio between inertial
321 force and frictional force. The comparison between Figure 10 and Figure 9b indicates that the
322 larger the ball size, the more collisional the flow mechanism would be. As a result, the inertial
323 forces dominate the flow dynamic compared with the frictional forces in the present tests.
324 Furthermore, the balls at the upper region of the flow associated with higher velocity had more

325 collisions and moved freely compared with that at the bottom region. The balls at the lower region
326 were compacted with lower flow velocities. By comparison, the numerical simulation results of
327 the flow pattern have a very good agreement with the physical test results when the micro-
328 parameters were selected suitably.

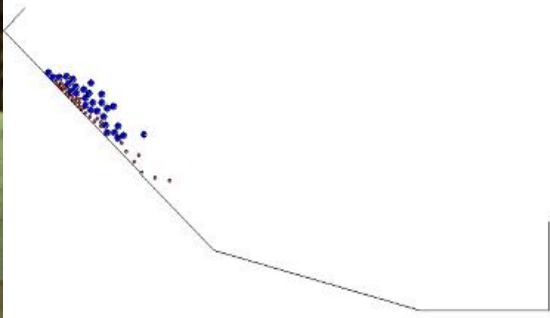
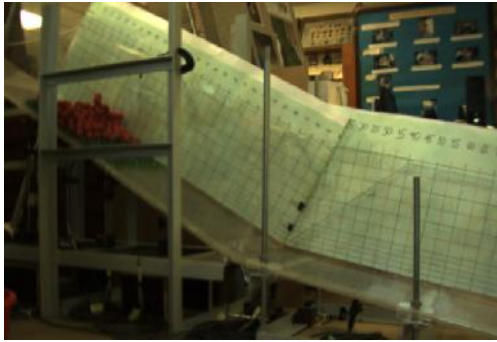
329 As shown in Figure 9b and Figure 10, segregation was also observed in the numerical model after
330 the dry granular balls started to move. In Figure 9b, it was evident that the blue balls with larger
331 ball size moved upwards and forwards, while the red balls with smaller ball size went to the lower
332 layer and stayed at the rear of the flow, which was consistent with the results in the physical model
333 tests. Smaller particles are more likely to move through the void between the larger particles, and
334 this will in turn squeeze the large particles to the upper layer of the flow. Because of the momentum
335 exchange between the balls and the flow mass dilation resulting from the shear deformation, a
336 dispersive pressure was caused which result in larger dry granular balls moved faster than the finer
337 particles and went upwards, and lead to the results that larger balls flowed to the upper layers
338 where the shear strain is low and accumulated at the front of the flow, while the finer balls tend to
339 moved downwards and accumulated at the bottom of the flow (Takahashi (1981)). Besides, the
340 difference of the ball size induce an unbalance forces on the balls which restrict the vertical
341 movement of the balls, this will also affects the flow segregation in the vertical direction.
342 Furthermore, the density difference between the balls the in numerical model is another factor that
343 influence the segregation process. Particles with lower density are more likely to rise to the free
344 surface while particles with higher density are more likely to segregate to the bottom of the flow.
345 From Figure 5b, it can be noticed that it is easily for the red balls with larger density traveled
346 through the gap generated by the shear deformation and squeezed the particle with smaller density
347 up to the upper flowing layer. The balls with higher density at the bottom pushed the balls with
348 smaller density forward. It is worth to mention that from the simulation results, the velocities of
349 the blue balls at free surface is the largest, which result in that the balls with large size migrated to
350 the front of the flow. The segregation mechanism simulated in the numerical model is in consistent
351 with what is aforementioned in the physical model tests. Ashwood and Hungr (2016), Choi et al.
352 (2014), Choi et al. (2015), Kwan (2012), Lo (2000), Ng et al. (2014), Ng et al. (2017) have
353 investigated the impact forces on the barrier which is however not considered in the present study,
354 as this is not the main theme of the present work.

355

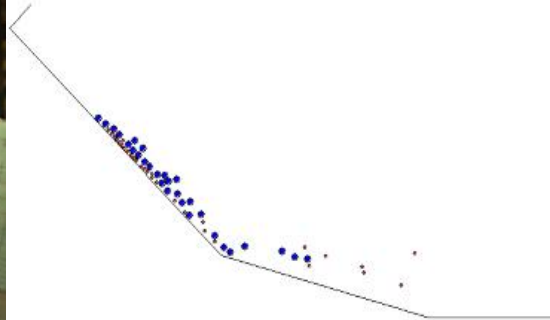
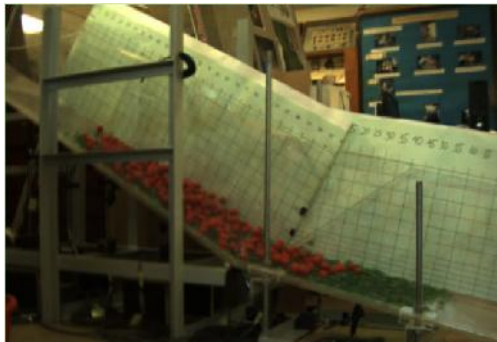


356

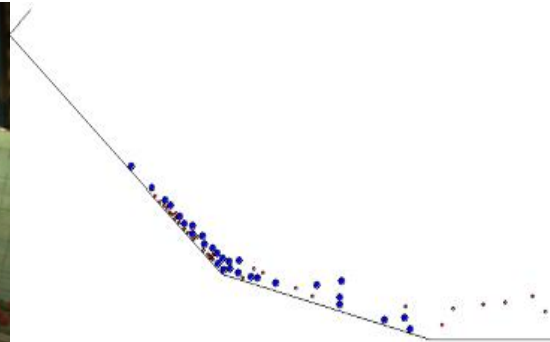
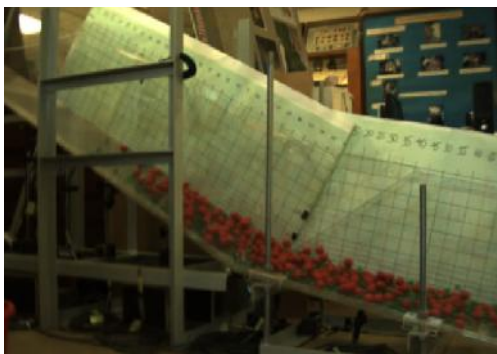
357



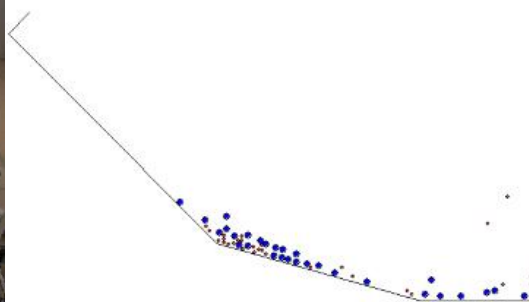
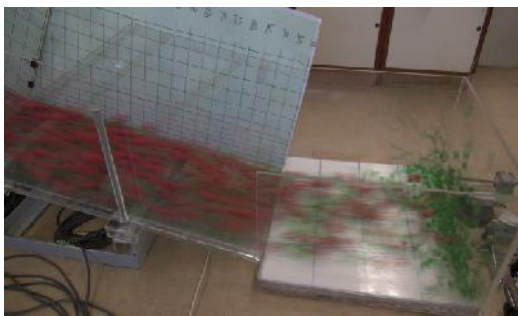
358

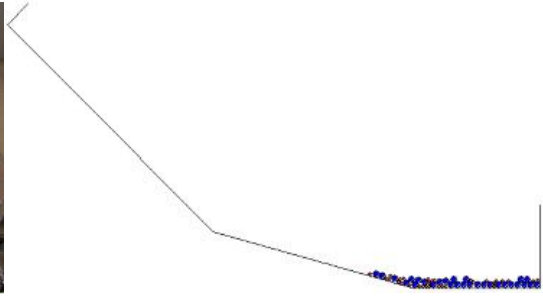
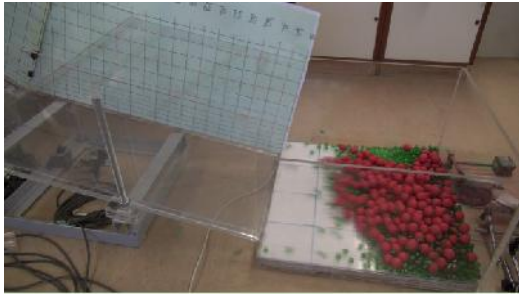


359



360





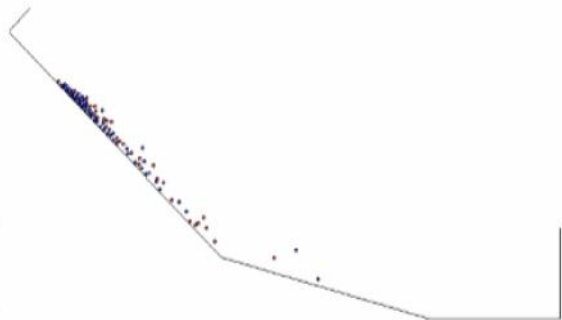
361

362 Fig. 9a. Flow pattern of multi-size
363 balls flow in physical test

Fig. 9. Flow pattern of multi-size
balls flow in numerical test

364 Fig. 9. Flow Pattern of multi-size particle flow composing of red plastic balls and green glass
365 balls

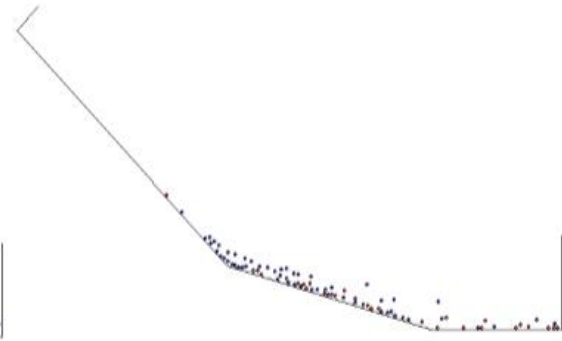
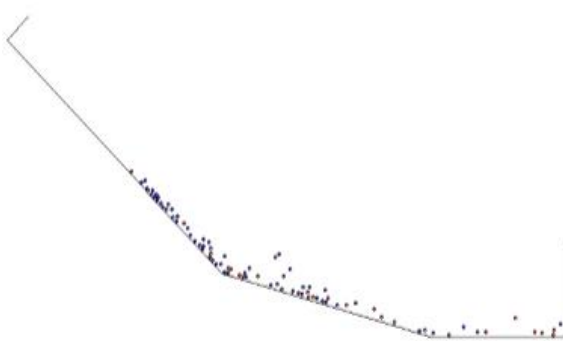
366



367

368 (a) Start of flow

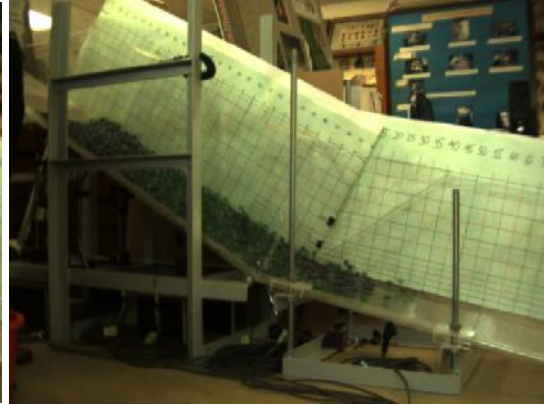
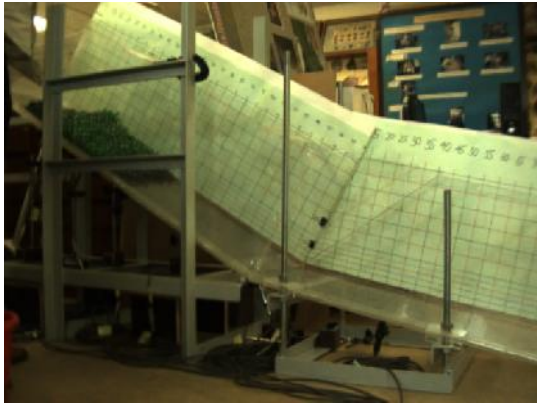
(b) 1/3 of flow time



369

370 (b) 2/3 of flow time

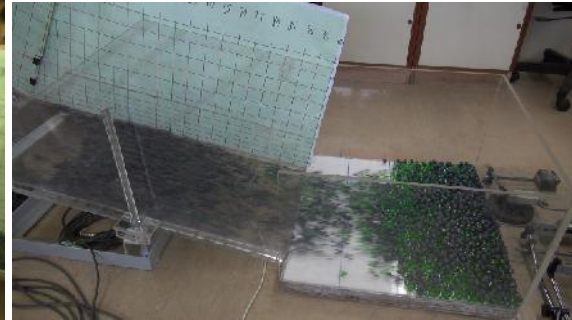
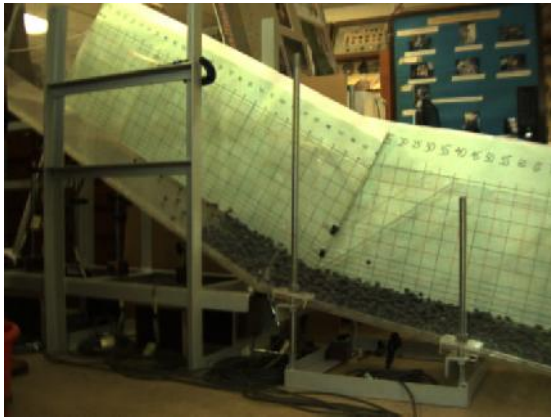
(d) end of flow



371

372 (e) Photo at start of flow

(f) photo at 1/3 of flow time



373

374 (g) photo at 2/3 of flow time

(h) photo at final stage

375

376 Figure 10. Flow Pattern of multi-size particle flow composing of black plastic
377 balls and green glass balls

378

379 3.3 The effect of the flume jump

380 To reduce the impact force and velocity of the granular flow mass, the authors have proposed to
381 add a jump in the flume as a pilot test in this study. From the results in this study, it is found that
382 the construction of a jump which has a very low cost has some small advantage in reducing the
383 impact from debris flow. Based on the present result, some rigid barriers in Hong Kong have
384 started to include a jump as a small benefit to the control of debris flow, and this is the reason for
385 carrying out such a test in the present research programme which is seldom considered in the past.
386 Figure 11 shows the numerical results of the flow pattern of the blue glass balls flowing on the
387 flume with or without a jump. The flow pattern of the blue glass balls flowing on the flume without
388 a jump in the numerical model is almost the same as the flow pattern of the red plastic balls in the

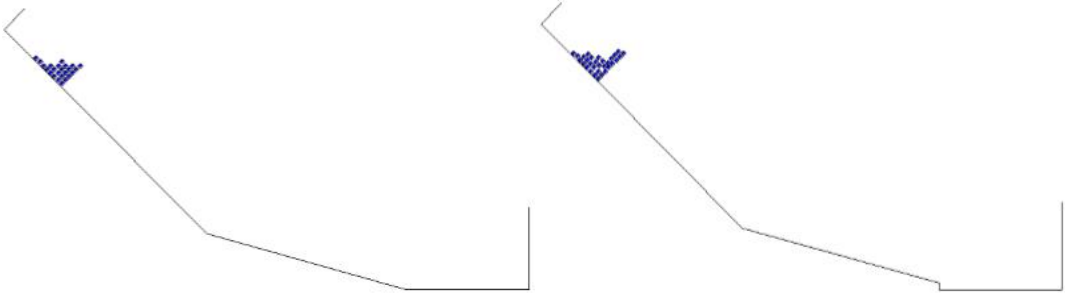
389 physical tests aforementioned. From the comparison of the flow pattern between Figure 11a and
390 Figure 11b, an important phenomenon was observed. The run up height of the balls flowing on the
391 flume with a jump is obviously lower than the run up height of the particles flowing on the flume
392 without a jump, which indicates that flume jump is able to facilitate the process of energy
393 attenuation and thereby has a good effect on suppressing the run up height of granular flow.

394 Figure 12 exhibits the velocity of the blue glass balls at different time step. In PFC2D, we have
395 developed the code to monitor the maximum velocity of the balls for comparison purpose, and the
396 monitored results are used to produce Fig.12. Black line represent the maximum velocity of the
397 blue glass balls with 10Kg weight flowing on the flume without a jump at different time step, while
398 the red line represent the same kind of balls with 13.55Kg weight on the flume with a jump. The
399 comparison of the velocities at point A and point B indicates that the peak velocity of the balls
400 flowing on the flume with a jump is pronouncedly smaller than that on the flume without a jump,
401 and the peak speeds of the balls on the flume with a jump were achieved earlier than balls on the
402 flume without a jump. It is worth to mention that the velocity of the balls is independent of the
403 mass of the test material, except that at the peak period.

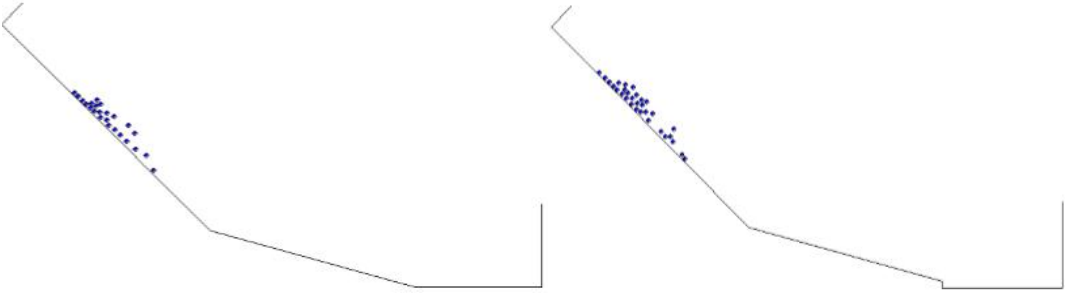
404 Figure 13 shows the velocity profile of mono-size particles (blue glass balls) along the flume with
405 or without a flume jump. The length of the velocity vector represents the speed of the particles.
406 From Figure 13, it can be noticed that the front flow velocities are the largest compared with the
407 velocities of the particles at the rear of the flow. When these particles approached the lower part
408 of the flume, the velocity directions changed due to the difference of the flume angles. This is in
409 good agreement with the laboratory results mentioned above. Figure 13b shows that the velocity
410 of mono-size particles on the flume with a jump increased after the initial state. The largest flow
411 velocity was achieved at the moment when these particles intend to jump into the deposition zone.
412 The directions of flow velocities changed and the speed of particles decrease as soon as they fell
413 into the deposition zone. As with those particles moving on the flume with a jump, the velocity of
414 the particles flowing along the flume without a jump increased when they approached the
415 deposition zone, however, the velocity of these particles kept increasing when they flowed into the
416 deposition area and the peak speed was achieved just before the moment when they reached the
417 boundary of the deposition area. When the granular front impacted on the wall of the deposition
418 area, these particles at the front of the flow reflect back and collide with the following particles,
419 and that is the moment when the flow speed decelerated.

420 According to Figure 12 and 13, the peak velocity of the balls on the flume with a jump achieved
421 before they impacted on the wall of deposition zone compared with that without a jump, which is
422 meaningful to the engineers because the flume jump can effectively reduce the impact force on the
423 barrier. Besides, the jump of the flume is capable of reducing the peak velocity of the dry granular
424 particle flow as well. To sum up, flume jump plays a useful role in attenuating granular flow,
425 therefore, flume jump is recommended to be applied in the design of debris flow barrier (which is
426 actually sometimes adopted in Hong Kong).

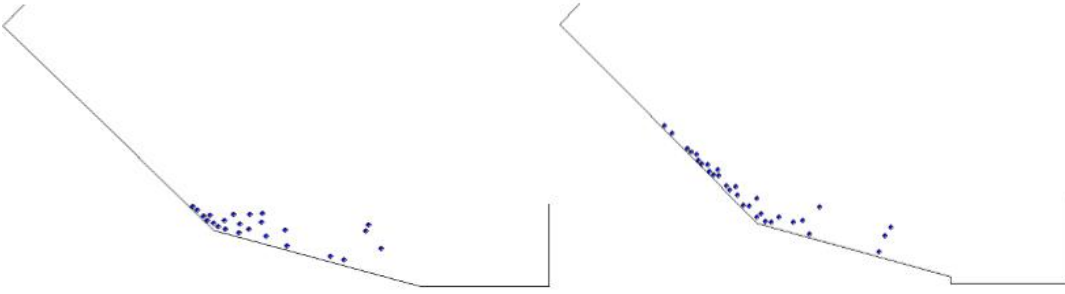
427



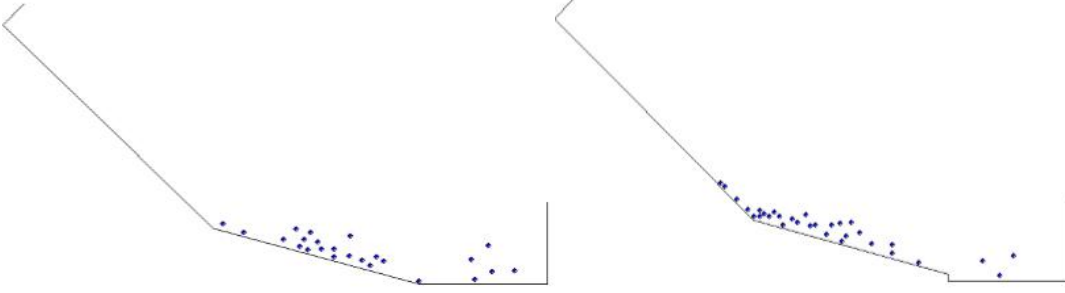
428



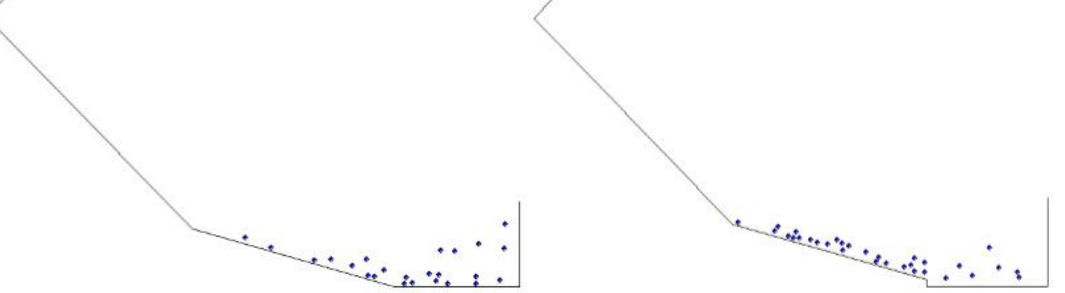
429



430

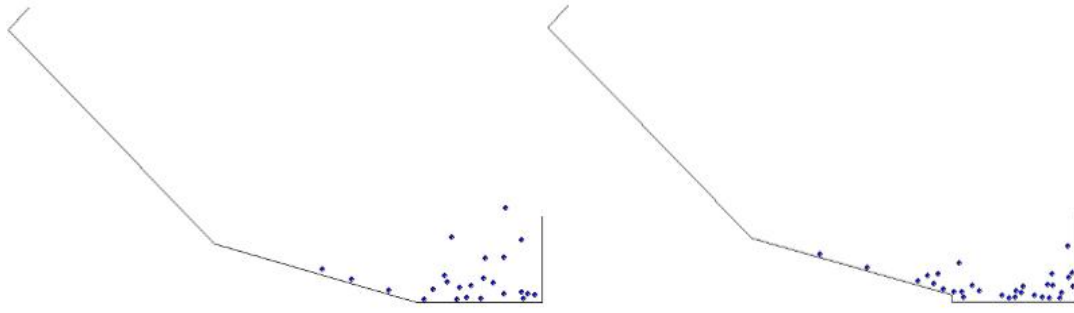


431

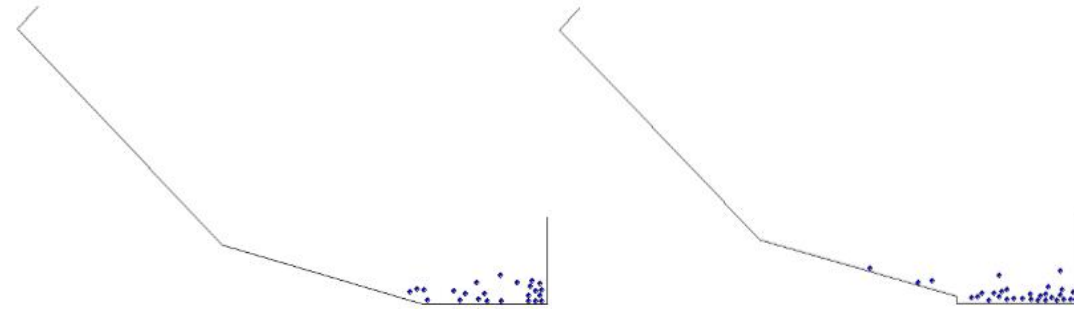


432

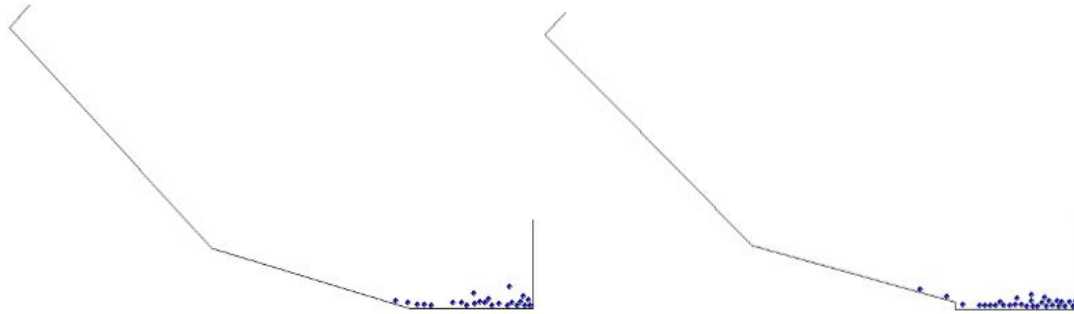
433



434



435

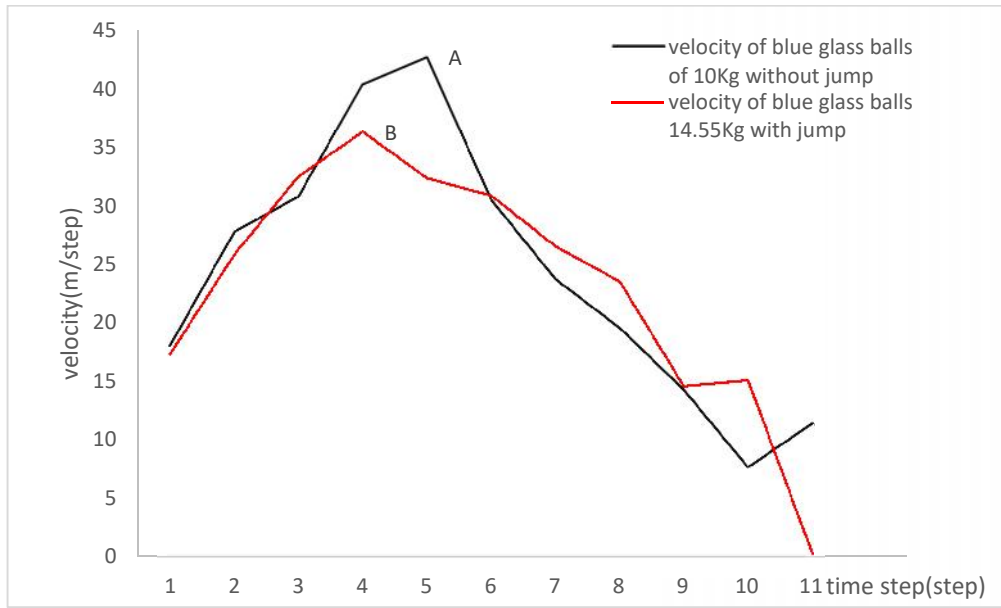


436 Fig. 11a. Flow pattern of blue glass balls
437 flowing along the flume without jump

436 Fig. 11b. Flow pattern of blue glass balls
437 flowing along the flume with jump

438 Fig. 11. Flow pattern of blue glass balls flowing on the flume with or without a jump

439



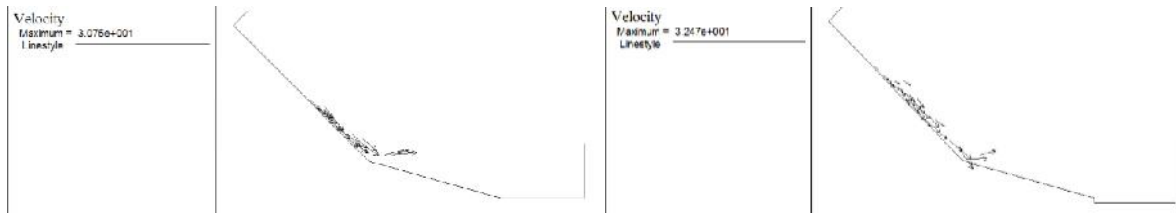
440

441

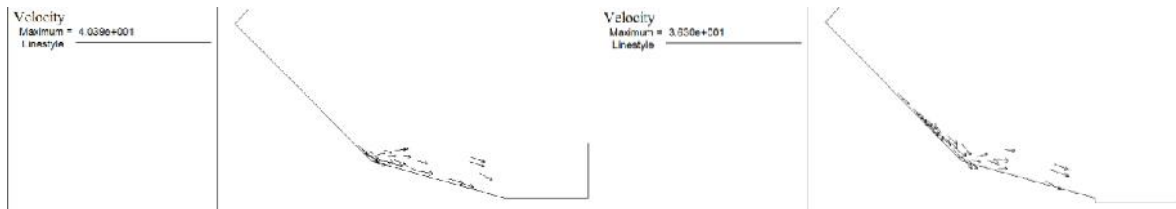
Fig. 12. Maximum velocity of blue glass balls in numerical model

442

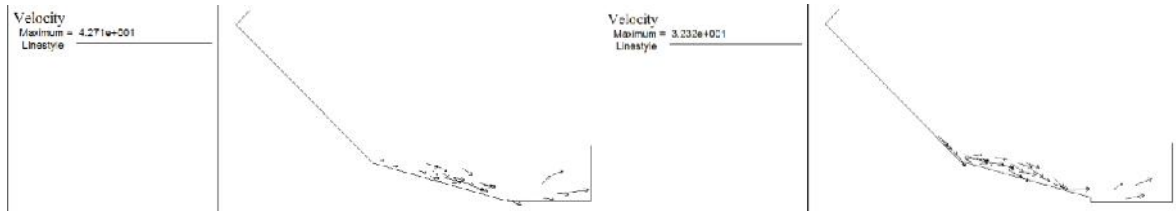
443



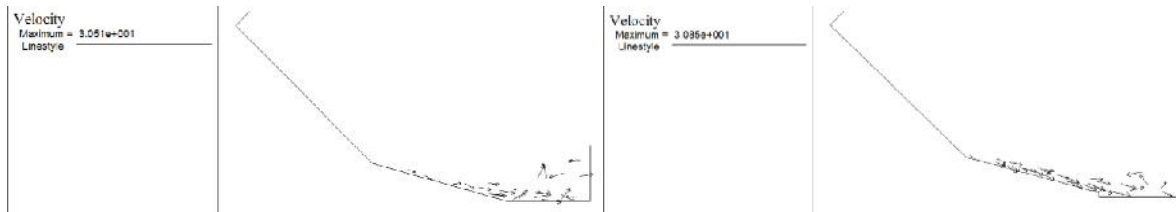
444

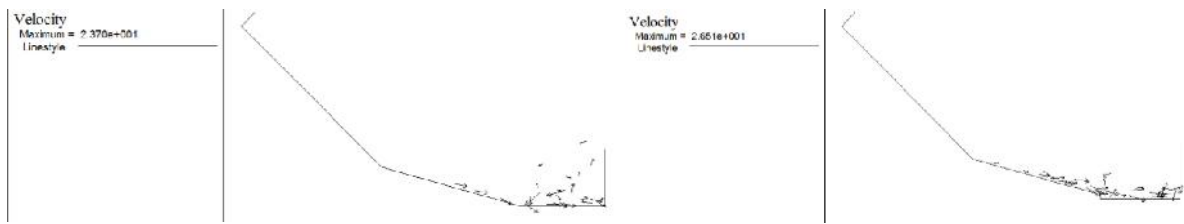


445



446





447
 448 Fig. 13a. Velocity profile of balls on the flume without a jump Fig. 13b. Velocity profile of balls on the
 449 flume with jump

450 Fig. 13. Velocity profile of blue glass balls in numerical model

451

452 It should be noted that the actual flow velocity of the balls can be traced back from the high speed
 453 camera photos and the movie, but we do not present the results here because it is not the main
 454 theme of the present study. Most importantly, DEM usually cannot give a good ~~for which~~
 455 quantitative prediction unless the micro-parameters are fine tuned. The authors do not prefer such
 456 tuning of the parameters, as such tuning cannot be performed before the tests. However, the
 457 qualitative results from the DEM analysis and the laboratory tests are reasonable as found from
 458 the present study, hence we can still accept the results from DEM in our discussion. Actually, the
 459 authors have carried out limited tuning of the micro-parameters (not shown in this paper) in our
 460 internal studies. Since the flow and segregation process are practically not affected by the change
 461 of these micro-parameters (but the actual value of the flow velocity, run-out ... are affected), we
 462 have not included these results in the present paper, and the authors prefer to concentrate on the
 463 segregation and jump for a flume test.

464

465 5. Large scale field tests

466 After the laboratory studies using a 1.5m long flume and glass/rubber balls, the authors have
 467 carried out a large scale flume test which is shown in Fig.14. The flume is about 6m long, and 5
 468 types of sand as shown in Fig. 15 are used in the field tests. The particle size within each type is
 469 relatively uniform, and they ranged from 1-3mm, 3-5mm, 5-7mm, 7-8mm and above 8mm. The
 470 friction angles for the 5 types of sand as determined from the deposition tests as shown in Fig.15b
 471 are given by 28°, 30.3°, 29.1°, 31.5° and 33.7° respectively.



472

473 Fig.14 Large scale flume for field test



474



475 Fig.15a Sand used for granular flow tests Fig.15b Deposition tests for sand

476

477 A series of tests with single, double and triple types of sand have been carried out, and only some
478 of the results are shown in this paper for comparisons with the laboratory tests. As shown in Fig.16,
479 the final deposition profile using type 1 (1-3mm) and type 4 (7-8mm) sands is shown. It is noticed
480 that the coarse grain sand move to the top of the flow, which are illustrated by Fig.17a to 17c. Such
481 results comply well with the laboratory studies. The control tests using coarse and finer sands are
482 shown in Fig.18. A closer look into the difference between Fig. 18a and Fig.16 is the profile at the
483 rear can reveal an important difference. For granular flow with 2 types of materials, the difference
484 in the height of deposit for the first meter as measured from the left is greater than that for the test
485 with single material (true for all single sand tests). Such phenomenon can be attributed to the effect
486 of the difference in the velocity flow between type 1 and 4 material, and type 1 material deposit at
487 the bottom during the flow. Based on the field tests, the importance of the particle size during the
488 segregation process as derived from the laboratory tests can be further verified.

489



490

491 Fig.16 Final deposition after the granular flow for two materials (coarse and fine)



492

493 Fig.17 a Deposition at the rear of the deposit



494 Fig.17b Deposition at the front of the deposit



495

496 Fig.17c Front view of the deposition (2 materials)

497



498

499 Fig.18a Front view of the deposition (type 4 material) Fig.18b Close up view of the deposition

500

501 With reference to Fig.19, it is clear that the formation of the flow front, flow head, channelized
502 flow and levee from the present field test is very similar to that by Johnson et al. (2012). The
503 surface trajectories of the particles by Johnson et al. (2012) are also captured by the high speed
504 camera in the present laboratory and field tests. A coarse enriched surface layer has been obtained
505 by Johnson et al. (2012), and such phenomena are also obtained from the laboratory and field tests
506 and is clearly illustrated in Fig.17. Iverson (1997) has also found similar segregation from the

507 granular flow at Oregon (1996). It should be noted that for all the granular flow tests in the present
508 study, such segregation phenomenon is always obtained, as long as there are more than 1 materials
509 in the problems.



510

511 Fig.19 Front of the runout

512 6. Discussion

513 Laboratory tests were carried with numerical simulations through distinct element method to study
514 the flow pattern of dry granular flow. The study is important for the basic understanding of the
515 granular flow segregation problem and the importance of providing a jump in the flume or in the
516 actual protective measures. For the present tests, the flume base is even and smooth which result
517 in relative small dynamic frictional angle and less energy attenuation compared with the real
518 granular flow. Besides, the surfaces of the glass and plastic balls used in the experiments are
519 regular and smooth, while for debris flow occurring in nature, the debris materials are always
520 irregular and rough, which cause the dynamic internal frictional shear force between real scale
521 debris flow particles are relatively large with a lower and hence the run up height is lower. As a
522 consequence, the present tests is a conservative test to study the flow pattern of granular flow.
523 Such arrangement is necessary so as to separate the contribution of particle size distribution from
524 other parameters in the segregation process.

525

526 Physical tests were conducted to study the flow pattern of mono as well as multiple size particle
527 flows. In general, the results from the present study comply well with those from the literature.
528 Test results indicate that flow mass elongated under the action of shear force during the particles
529 flowed on the flume. For multi-size particles with different particle sizes, segregation always
530 occurs. Particles with larger diameters migrated upward and small particles moved downwards

531 because particles with smaller diameter can go through the gap between the larger particles. In
532 addition, the density of the particle is another factor that play a role in the segregation process.
533 Under the action of gravity, particles with higher density moved downwards faster and other
534 particles with lower density were squeezed up. For the real scale debris flow, the debris material
535 ranges from clay and silt to boulders while the differences in the densities between different types
536 of particles are relatively small, hence particles size will be the most dominant factor which
537 influence the segregation process. The top view from high speed camera indicates that the
538 velocities of the large particles are higher than the velocities of the small particles. Granular
539 particles with larger particles sizes travelled to the front of the flow where the velocities are higher.
540 Larger particle size is observed to lead to a higher velocity. Such results are also in general
541 agreement with the results by Takahashi (1980).

542

543 For the present work, the detailed movement of individual particle is hard to trace even with the
544 help of high speed camera. Instead of that, the authors choose to trace the segregation process
545 through the macro phenomena such as grain migration, segregation and the formation of the levee.
546 Combined with the DEM analysis, the interpretation of individual grain movement as well as the
547 formation of the segregation and levee can be assessed. Based on the various laboratory and field
548 tests on flow with mixture of different material sizes, stiffness and density, it is established that
549 the grain size distribution is the most critical factor in the flow process, as grain movement occur
550 and control the flow process at about half of the flow process. The formation of the force chain
551 which actually affect the flow process is also controlled by the grain size distribution. This result
552 has an important implication in that most of the natural flow process involve debris of different
553 grain sizes.

554

555 For the flow pattern of dry granular particles simulated through distinct element method, the
556 simulation results of flow pattern are almost the same as the physical tests. Berger (2016), Chen
557 and Lee (2000), Ghilardi et al. (2001) also obtained a reasonably well numerical modeling of the
558 flow process for relatively simple flow problem which support the use of numerical analysis for
559 the granular flow problem. In the present numerical model, a pronounced segregation process was
560 observed as well, which comply well with many previous studies by Gray et al. (2003),
561 Hákonardóttir et al. (2003), Iverson (1997), Johnson et al. (2012) and many others. Large particles
562 went upwards while small particles went downwards. From the velocity vector figure, the
563 velocities of the particles at upper layer as well as the velocities at the front of the flow were the
564 largest. Savage numbers of the dry granular particles in present tests were larger than 0.1, which
565 represent the collisional character of the flow. The flow behavior was hence more inertial than
566 frictional. Flume jump have a significant influence on the impeding granular flow. When the
567 particles flowed through the jump a large quantity of kinetic energy were consumed during this
568 process. The peak velocities of particles flowing on the flume with a jump were lower than that
569 without a flume jump. Besides, the peak velocities of the particles on the flume with a jump were
570 achieved earlier, and after that the flow velocity started to decrease, which would make a great
571 contribution for reducing the impact load. The run up height of the particles on the flume with a

572 jump was apparently lower than that without a jump. Thus, flume jump can help to reduce the flow
573 velocity as well as suppress the run up height. In previous sections, detailed discussion about the
574 formation of force chain from DEM are investigated, and such force chain has a major effect to
575 the flow and segregation process which is actually observed from the tests. Without the DEM
576 results, these phenomenon cannot be explained clearly. In this respect, the use of numerical
577 modelling has provided an important help to the understanding of the flow and segregation process.

578 Comparing the physical and numerical test results, the macroscopic flow behavior in numerical
579 models are consistent with the physical tests. Through a good selection of the model generation
580 method and micro parameters, the distinct element method can produce a reasonable qualitative
581 simulation of the behavior of dry granular flow for the consideration of the engineers. These results
582 have useful contributions to the better understanding of the granular flow behavior which is not
583 possible for the other classical methods. Up to the present, the engineers are still relying on some
584 empirical methods such as dynamic impact earth pressure coefficient (Kwan 2012) or similar
585 approaches for the design of flexible or rigid barrier, as granular flow process is complicated by
586 many geotechnical and geographical complexities. The design of the barrier is still more an art
587 than science up to the present, though some guidelines are available to help the engineers in the
588 design. However, The DEM analysis in this study can supplement the field and laboratory studies
589 for which the internal forces between the particles cannot be determined.

590

591 The flow process and segregation process from laboratory and field tests are similar in many
592 respect – largely controlled by the particle size distribution. This is clearly illustrated from about
593 50 tests in our study. Limited photos are shown in this paper to limit the length of the paper.
594 Thousands of photos and about a hundred movie files are obtained from the laboratory and field
595 tests in this study, and only selected photos which are sufficient to illustrate the main purposes of
596 the present work are shown in the present paper. The authors are however happy to share these
597 materials upon request at cymchen@polyu.edu.hk.

598

599 In the present paper, the effect of the flume inclination has not been investigated. Actually, the
600 authors have carried out some tests on the effects of flume inclination. For the segregation process,
601 the test results indicate that the basic conclusions from the present work remains unchanged, for
602 practical purposes. Flume inclination has more important effects on the impact forces and erosion
603 which are to be covered by the next stage of the present research work.

604

605 **7. Conclusion**

606 In the present study, two important phenomena in granular flow are studied. The first problem is
607 the segregation process which is captured in all the tests in the present studies. The segregation
608 phenomenon can affect the design of the barrier in different ways. The finer materials will be
609 deposited at the bottom of the runout, and the relatively lower permeability of this layer will tend
610 to drive the water level upward (somewhat similar to the perch water table phenomenon). This

611 may increase the destructive power of water. For the design of rigid barrier, the use of a suitable
612 water table will also be crucial to maintain adequate factor of safety of the barrier. Since
613 segregation will occur practically for majority of the debris flow problems, this effect should be
614 well studied and considered in the design of flexible and rigid barriers.

615

616 The authors have chosen flexible spherical rubber beads as well as rigid glass beads for the
617 laboratory, and the range of stiffness would be sufficient to cover most of the natural flow materials.
618 The segregation process as found from the laboratory test is actually similar to that in the field
619 tests using non-spherical sand. Through such selection, it is clearly demonstrated that particle size
620 distribution is a very critical factor in the segregation process, and it appears that it is more critical
621 than particle shape or stiffness.

622

623 To reduce the destructive power of the debris, a small jump in the flow channel is sometimes
624 applied in Hong Kong if the site condition allow. In general, the effect of this jump is small, and
625 is effective only for small volume debris flow which is the common case for Hong Kong.
626 Nevertheless, such provision can slightly reduce the destructive power of the debris. It is
627 interesting to note that there is virtually no study about the effect of the jump in the past, and the
628 present work provide some useful pilot works, for which more works may come out in the future.

629

630 One of the main limitations for the present study is that the flow material is limited to granular but
631 not cohesive material. The reason is that all debris flows in Hong Kong are practically granular
632 debris flows. The most critical factors in debris flow for Hong Kong include also different particle
633 size distribution (studied in the present work), topography and the effects of water. The present
634 work do not aim to consider all these effects simultaneously, but is confined to address the critical
635 issues as found in Hong Kong. Nevertheless, the present work will still be useful to many countries
636 where the flow material is mainly granular.

637

638 The authors are currently considering the next stage of field tests, for which the wet test will be
639 carried out (limited tests have been so far), and more equipment and measurements will also be
640 used. Currently, the authors are constructing a laboratory flume where the base is rough. The
641 combined effect of base roughness and flume inclination angle will be carried out soon, and
642 hopefully the results will form the extension of the present paper. For the field test, most of the
643 researchers place a contained of wet sample and let the sample flow down. This approach is simple
644 to be executed, but the actual debris flow may not be like that. From the observations of several
645 debris flows in Hong Kong, the authors have noticed that erosion process is sometimes an
646 important phenomenon which is not simple to be reproduced in the field flume. The composition
647 of the flow material actually changes during the flow process. More thoughts will be given to the
648 setup of the wet field test in the future, and the base of the flume may be specially prepared with
649 some soil bedding to allow for erosion in the future tests.

650

651 **Acknowledgement**

652 The present project is funded from the Research Grants Council of the Hong Kong SAR
653 Government through the project PolyU 152293/16E, and CityU University of Hong Kong
654 Research Project No. 7004631, National Natural Science Foundation of China (Grant No.
655 51778313) and Cooperative Innovation Center of Engineering Construction and Safety in
656 Shangdong Blue Economic Zone.

657

658 **Reference**

659 Ashwood, W., & Hungr, O. (2016). Estimating total resisting force in flexible barrier impacted
660 by a granular avalanche using physical and numerical modeling. *Canadian Geotechnical Journal*,
661 53(10), 1700-1717.

662 Berger C. (2016), A comparison of physical and computer-based debris flow modelling of a
663 deflection structure at Illgraben, Switzerland, INTERPRAEVENT 2016, 212-220.

664 Chan, C. P. L. (2001), Runout distance of debris flows: experimental and numerical simulations
665 (Doctoral dissertation, The Hong Kong Polytechnic University).

666 Chen H. and Lee C.F. (2000), Numerical simulation of debris flow, *Canadian Geotechnical*
667 *Journal*, 37:146-160.

668 Cheng Y.M., Liu H.T. and Au S.K. (2005), Location of critical three-dimensional non-spherical
669 failure surface with applications to highway slopes, *Computers and Geotechnics*, no. 32, 387-399.

670 Cheng YM, Li N. and Yang XQ (2015), Three Dimensional Slope Stability Problem with a
671 Surcharge Load, *Natural Hazards And Earth System Sciences*, 15(10), 2227-2240.

672 Choi, C. E., Au-Yeung, S. C. H., Ng, C. W., & Song, D. (2015), Flume investigation of landslide
673 granular debris and water runup mechanisms. *Géotechnique Letters*, 5(1), 28-32.

674 Choi, C. E., Ng, C. W., Song, D., Kwan, J. H. S., Shiu, H. Y. K., Ho, K. K. S., & Koo, R. C. H.
675 (2014). Flume investigation of landslide debris-resisting baffles. *Canadian Geotechnical Journal*,
676 51(5), 540-553.

677 Coussot, P. and Meunier, M, (1996), Recognition, classification and mechanical description of
678 debris flows, *Earth-Science Reviews*, 40: 209–227.

679 Cruden,D.M. and Varnes, D.J., (1996), *Landslide Types and Processes*, Special Report ,
680 Transportation Research Board, National Academy of Sciences, 247:36-75

681 Cundall, P. A. (1971), A computer model for simulating progressive large scale movements in
682 blocky rock systems. In *Proc. Symp. Rock Fracture (ISRM)*, Nancy, France, 129-136.

683 Cundall P A. (1988), Formulation of a three-dimensional distinct element model—Part I. A
684 scheme to detect and represent contacts in a system composed of many polyhedral blocks,

685 International Journal of Rock Mechanics and Mining Sciences & Geomechanics Abstracts.
686 Pergamon, 25(3): 107-116.

687 Cundall, P. A. and Hart, R. D. (1992), Numerical modelling of discontinua. Engineering
688 Computations, 9(2), 101-113.

689 Cundall, P. A. and Strack, O. D. (1979), A discrete numerical model for granular assemblies.
690 Geotechnique, 29(1), 47-65.

691 Furuya, T., 1980, Landslides and landforms: in Landslides, slope failures and debris flows
692 (Takei, A. ed.), Kajima Shuppan, Tokyo, pp.192–230.

693 Ghilardi P., Natale L. and Savi F. (2001), Modeling debris flow propagation and deposition,
694 Phys. Che. Earth 9:951-656.

695 Gray, J. M. N. T., Tai, Y. C., & Noelle, S. (2003), Shock waves, dead zones and particle-free
696 regions in rapid granular free-surface flows. Journal of Fluid Mechanics, 491, 161-181.

697 Hákonardóttir, K. M., Hogg, A. J., Batey, J., & Woods, A. W. (2003), Flying avalanches.
698 Geophysical Research Letters, 30(23).

699 Halsey and Mahta (2002), Challenges in Granular Physics, World Scientific

700 Hungr, O. (1995), A model for the runout analysis of rapid flow slides, debris flows, and
701 avalanches, Can. Geotech. J., 32, 610–623.

702 Hungr O., Evans S.G., Bovis M. and Hutchinson J.N. (2001), Review of the classification of
703 landslides of the flow type, Environmental and Engineering Geoscience, VII, 221-238.

704 Hutter, K., Wang, Y., & Pudasaini, S. P. (2005), The Savage–Hutter avalanche model: how far
705 can it be pushed? Philosophical Transactions of the Royal Society of London A: Mathematical,
706 Physical and Engineering Sciences, 363(1832), 1507-1528.

707 Iverson, R. M., Reid, M. E., & LaHusen, R. G. (1997), Debris-flow mobilization from landslides
708 1. Annual Review of Earth and Planetary Sciences, 25(1), 85-138.

709 Iverson, R. M., & LaHusen, R. G. (1989), Dynamic pore-pressure fluctuations in rapidly
710 shearing granular materials. Science, 246(4931), 796-800.

711 Iverson, R. M., & LaHusen, R. G. (1993), Friction in debris flows: Inferences from large-scale
712 flume experiments. American Society of Civil Engineers (Ed.), Hydraulic Engineering, 93.

713 Iverson R.M. (1997), The physics of debris flows, Reviews of Geophysics, 35(3):245-296.

714 Iverson, R.M., and George, D.L., (2016), Discussion of “The relation between dilatancy,
715 effective stress and dispersive pressure in granular avalanches” by P. Bartelt and O. Buser, Acta
716 Geotechnica, 11(6), 1465-1468

717 Jakob M. and Hungr O. (2005), Debris flow hazards and related phenomena, Springer Praxis.

718 Jiang, M., J. Konrad, and S. Leroueil (2003), An efficient technique for generating homogeneous
719 specimens for DEM studies, *Computers and Geotechnics* 30, 579–597.

720 Johnson A.M. (1996), A model for grain flow and debris flow, U.S. Department of the Interior
721 U.S. Geological Survey, Open-file-report 96-728.

722 Johnson C.G., Kokelaar B.P., Iverson R.M., Logan M., LaHusen R.G. and Gray J.M.N.T.
723 (2012), Grain-size segregation and levee formation in geophysical mass flows, *Journal of*
724 *Geophysical Research*, 117, F01032.

725 Kesseli, J. E. (1943), Disintegrating soil slips of the Coast Ranges of Central California. *The*
726 *Journal of Geology*, 51(5), 342-352.

727 Scott K. M. and Wang Y.Y. (1997), Debris flow - Geological process and hazard illustrated by a
728 surge sequence at Jiangjia ravine, Yunnan, China, U.S. Geological Survey Professional Paper
729 1671.

730 King J.P. (2013), Tsing Shan Debris Flow and Debris Flood, GEO Report No. 281, Hong Kong
731 SAR Government.

732 Kwan, J. S. H. (2012). Supplementary technical guidance on design of rigid debris-resisting
733 barriers. Geotechnical Engineering Office, HKSAR. GEO Report, (270).

734 Li K.H. (2013), Laboratory debris flow flume test, Hong Kong Polytechnic University.

735 Lin, D. G., Hsu, S. Y., & Chang, K. T. (2009), Numerical simulations of flow motion and
736 deposition characteristics of granular debris flows. *Natural hazards*, 50(3), 623-650.

737 Liu, X. (1996), Size of a debris flow deposition: model experiment approach. *Environmental*
738 *Geology*, 28(2), 70-77.

739 Lo, D. O. K. (2000), Review of natural terrain landslide debris resisting barrier design. HKSAR:
740 GEO, Report no. 104.

741 Lo, K. H. (2004), Theoretical simulations of debris flow and their applications to hazard
742 mapping using GIS (Doctoral dissertation, The Hong Kong Polytechnic University).

743 Lo O.K., Law H.C., Wai C.T., K.L. Ng, Williamson S.J., Lee K.S. and Cheng Y.M. (2018),
744 Investigation of an unusual landslide at Sai Kung Sai Wan Road, Sai Kung, HKIE Transaction
745 Theme issue on landslides and debris flow, 102-114.

746 Major, J. J. (1997), Depositional processes in large-scale debris-flow experiments. *The Journal*
747 *of Geology*, 105(3), 345-366.

748 Mancarella D. and Hungr O. (2010), Analysis of run-up of granular avalanches against steep,
749 adverse slopes and protective barriers, *Canadian Geotechnical Journal*, 2010, 47(8): 827-841

750 McDougall and Hungr (2004), A model for the analysis of rapid landslide motion across three-
751 dimensional terrain, *Canadian Geotechnical Journal*, 41(6): 1084-1097

752 Mizuyama, T., Uehara.S. (1983), Experimental study of the depositional process of debris flows.
753 Trans. Jpn. Geomorph. Union 4, 39-64.

754 Ng, C. W. W., Choi, C. E., Kwan, J. S. H., Koo, R. C. H., Shiu, H. Y. K., & Ho, K. K. S. (2014),
755 Effects of baffle transverse blockage on landslide debris impedance. *Procedia Earth and*
756 *Planetary Science*, 9, 3-13.

757 Ng, C. W. W., Choi, C. E., Liu, L. H. D., Wang, Y., Song, D., & Yang, N. (2017), Influence of
758 particle size on the mechanism of dry granular run-up on a rigid barrier. *Géotechnique Letters*,
759 7(1), 79-89.

760 Ohyagi, N., 1985, Definition and classification of sediment hazards: in *Prediction and*
761 *countermeasures of sediment hazards* (Japanese Soc.Soil Mech. Foundation Eng. ed.), Japanese
762 Soc. Soil Mech. Foundation Eng., Tokyo: 5–15.

763 Pierson, T.C. and Costa, J.E., 1987, A rheologic classification of subaerial sediment-water flows:
764 in *Debris flows/avalanches: process, recognition, and mitigation* (Costa, J.E. and Wieczorek,
765 G.F. eds.), *Rev. Eng. Geol.*, 7, Geolo. Soc. Am: 1–12.

766 Pudasaini S.P., Wang Y. and Hutter K. (2005), Modelling debris flows down general channels,
767 *Natural Hazards And Earth System Sciences*, 5, 799-819.

768 Pudasaini & Hutter (2007), *Avalanche Dynamics, Dynamics of Rapid Flows of Dense Granular*
769 *Avalanches*, Springer Verlag.

770 Rodine, J. D., Johnson, A. M., & Rich, E. I. (1974), *Analysis of the mobilization of debris flows.*
771 *Stanford University California, Department of Geology.*

772 Rodolfo, K. S., Umbal, J. V., Alonso, R. A., Remotigue, C. T., Paladio-Melosantos, M. L.,
773 Salvador, J. H. and Miller, Y. (1996), Two years of lahars on the western flank of Mount Pinatubo:
774 Initiation, flow processes, deposits, and attendant geomorphic and hydraulic changes. *Fire and*
775 *mud: eruptions and lahars of Mount Pinatubo, Philippines*, 989-1013.

776 Mizuyama, T., & Uehara, S. (1983), Experimental study of the depositional process of debris
777 flows. *Japanese Geomorphological Union*, 4(1), 49-63.

778 Savage, S. B. and Hutter, K. (1989), The motion of a finite mass of granular material down a
779 rough incline, *J. Fluid Mech.*, 199, 177–215.

780 Savage S.B. and Lun C.K.K. (1988), Particle size segregation in inclined chute flow of dry
781 cohesionless granular soils, *J. Fluid Mech.*, 199, 177-215.

782 Sullivan, C. (2011), *Particulate discrete element modelling*. Taylor & Francis.

783 Takahashi, T. (1981), Debris flow. *Annual review of fluid mechanics*, 13(1), 57-77.

784 Takahashi, T., (2001), Mechanics and simulation of snow avalanches, pyroclastic flows and
785 debris flows, *Spec. Publs., Int. Ass. Sediment*, 31: 11–43.

- 786 Takahashi, T., (2006), Mechanisms of sediment runoff and countermeasures for sediment
787 hazards, Kinmirai Sha.
- 788 Takahashi T. (2014), Debris Flow - Mechanics, Prediction and Countermeasures, 2nd edition,
789 CRC Press.
- 790 Varnes, D.J., (1978), Slope movement types and processes: in Landslides analysis and control
791 (Scguster, R.L and Krizek, R.J. eds.), NAS Sp. Rep. 176: 11–33.
- 792 Voellmy, A. (1955), Über die Zerstörungskraft von Lawinen. Schweizerische Bauzeitung 73,
793 159–162, 212–217, 246–249, 280–285. In German.
- 794 Wong W.L. (2018), Debris flow analysis by meshless method for Shum Wan Road landslide,
795 degree report, Hong Kong Polytechnic University
- 796 Yamashiki Y., Mohd Remy Rozainy M.A.Z.c, Matsumotod T., Takahashie T. and Takarabc K.
797 (2013), Particle Routing Segregation of Debris Flow Mechanisms Near the Erodible Bed,
798 Procedia APCBEE, 527-534.
- 799 Zohdi, T. I. (2007), P-wave induced energy and damage distribution in agglomerated granules
800 Modelling and simulation in materials science and engineering. 15, S435-S448.
- 801 Zhou G.D., Law R.P.H. & Ng C.W.W. (2009), The mechanisms of debris flow: a preliminary
802 study, Proceedings of the 17th International Conference on Soil Mechanics and Geotechnical
803 Engineering, 1570-1573.